Conjugated Polymers of Intrinsic Microporosity (C-PIMs)

*Ge Cheng, Baltasar Bonillo, Reiner S. Sprick, Dave J. Adams, Tom Hasell, and Andrew I. Cooper**

Conjugated microporous polymers (CMPs) have shown great potential for energy and environmental issues, however, poor solubility and processability of most of these materials limit their applications. Herein, a range of linear conjugated polymers of intrinsic microporosity (C-PIMs) is reported, combining for the first time the properties of conjugated microporous polymers, such as tunable electronic properties and compositional variation, with those of linear polymers of intrinsic microporosity (PIMs) allowing for solution processability and film formation. These soluble materials have a number of potential applications, for example as components in devices where large, porous interfaces are combined with extended electronic conjugation.

1. Introduction

Synthetic organic polymers with pores of molecular dimensions have emerged as an important platform in materials chemistry. They have applications, for example as adsorbents and as membranes for gas separation. In 2007, we reported the synthesis of conjugated microporous polymers (CMPs), the first networks to combine permanent microporosity (pores < 2 nm) with extended π-conjugation.[1] Subsequently, CMPs have been explored in catalysis,[2] light-harvesting,[3] carbon dioxide capture,[4] superhydrophobic separations,[5] luminescence,[6] sensing,[7] and energy storage.[8] Most CMPs and related networks are based on aromatic monomers and are prepared by carbon-carbon coupling, whereby high surface areas of up to 6500 m^2 g^{-1} can be achieved.[9] However, the complete lack of solubility of these networks limits the scope for some of the more interesting applications of CMPs. It is still difficult to process insoluble CMP networks into thin films, even though a few methods now exist, such as emulsion techniques involving solution-dispersible CMP nanoparticles,[10] and a two-step process involving thermal treatment trimerization of aromatic nitriles.[11] In this paper, we show that a range of linear, solution-processable conjugated polymers can also exhibit permanent microporosity, and that these can be considered as a subclass of PIMs[12] that we refer to here as "conjugated polymers of intrinsic microporosity" (C-PIMs).

Previously, we combined intrinsic porosity, conjugation, and solution processability in one system by developing soluble conjugated microporous polymers,[13] or "SCMPs", which comprise discrete hyperbranched chains. Effectively, these hyperbranched chains represent subunits of an extended CMP network, and they are hence soluble in common solvents. SCMPs can be solution-processed to form films, and their porosity can be tuned according to the processing conditions. In general, rapidly precipitated materials have higher surface areas than slowly precipitated materials because the pore structure is "locked-in" rather than being able to relax into a less porous state. This can be exploited to control the gas selectivity of the materials.

These branched SCMPs, which were all based on pyrene monomers,[13] have rigid structures that pack inefficiently in the solid state, as also observed for polypyrene dendrimers[14] and linear polypyrenes.[15] For example, aggregation and excimer emission are suppressed in organic light-emitting films as a result of the large dihedral angle between the 1,3-substituted pyrene units.

Our first-generation SCMPs were all branched, but linear, soluble organic polymers can also be porous. The best known example is the polymer of intrinsic microporosity, PIM-1, which has a Brunauer-Emmett-Teller (BET) surface area (SA_{BET}) of around 700 m^2 g^{-1}.[12] This microporosity stems from the rigid but contorted backbone in PIM-1, which promotes inefficient packing in the solid state.[16] Thus far, most PIMs have comprised a rigid ladder structure linked by cyclic di-ethers, combined with groups that introduce a site of contortion to disrupt close-packing, such as spirobisindane,[17] hexaphenylbenzene (HPB),[18] triptycene derivatives,[19] bowl-shaped monomers,[20] or calix[4]resorcinarene derivatives.[20] PIMs can be processed from solution into microporous films and coatings for applications such as nanofiltration, pervaporation, and gas separation. However, no extended π-conjugation exists in the backbones of these ladder PIMs. Given the strong interest in solution-processable conjugated polymers in organic photovoltaics[21] and related applications,[22] we initiated a search for linear "conjugated PIMs" (C-PIMs): that is, linear polymers that might combine

Dr. G. Cheng, Dr. B. Bonillo, Dr. R. S. Sprick, Dr. D. J. Adams, Dr. T. Hasell, Prof. A. I. Cooper
Department of Chemistry and Centre for Materials Discovery
University of Liverpool
Crown Street, Liverpool L69 3BX, UK
E-mail: aicooper@liv.ac.uk

DOI: 10.1002/adfm.201401001

Table 1. Molecular weight and apparent BET surface areas for the polymers.

Polymer	M_w [g mol^{-1}][a)]	M_n [g mol^{-1}][a)]	PDI	SA_{BET} [m^2 g^{-1}][b)]
A	2360	1850	1.28	400
B	4670	3910	1.19	573
C	4910	3970	1.24	628
D	8140	6350	1.28	728
E	26 300	9900	2.66	646
F	4450	3480	1.28	492
G	31 300	14 200	2.21	492
H	104 000	11 200	9.29	724
I	4860	3950	1.23	460
J	14 300	9070	1.57	585
K	3940	3170	1.24	322
L	8150	5010	1.63	552
M	1 740 000	1 040 000	1.67	436
N	1 910 000	1 410 000	1.35	470
O	92 700	50 900	1.82	438
P	190 000	63 900	2.97	[d)]
Q	22 900[c)]	16 200[c)]	1.41	293
R	23 000[c)]	17 800[c)]	1.29	[d)]

[a)]For GPC conditions, see Supporting Information; [b)]Gas sorption data given for the antisolvent precipitated form; Apparent BET surface area calculated over range P/P_0 = 0.01–0.1; [c)]THF-soluble fraction; [d)]non-porous. An example mass spectrum of fragmentation, for polymer **D**, is shown in Figure S1, Supporting Information.

porosity and conjugation with the solution processability required for device fabrication.[23]

We report here a range of linear C-PIMs. The chemistry encompasses both metal-mediated carbon-carbon bond formation, as for most CMP networks,[1–9] and also metal-free polycondensation routes, such as Diels-Alder polycondensation. By studying some of these polymers over a range of molecular weights, we find a roughly linear relationship between the chain length and apparent BET surface area.

2. Results and Discussion

Polymers **A–L** (**Table 1**, **Scheme 1**; also Scheme S1, Supporting Information) were synthesized using transition metal Pd- or Ni-mediated polymerizations (Suzuki coupling[24] and Yamamoto coupling[25]) or by a metal-free Diels-Alder approach (polymers **G–J**). The latter is potentially attractive from a cost perspective.[26] Linear 1,3-polypyrenes (**A–D**) were obtained at different molecular weights (Table 1) depending on the polymerization conditions (see Scheme 1, Supporting Information). Polymers **A** and **C** were prepared by Suzuki polymerization, and polymers **B** and **D** using Yamamoto coupling. Polymers **E**, **F**, **K**, and **L** were prepared via polycondensation of pyrene boronic acid pinacol ester with the appropriate dibromo-substituted comonomer. Metal-free polymerization based on Diels-Alder addition of biscyclopentendienone and bisalkynes in diphenylether gave polymers **G–J**. We also synthesized a further range of linear conjugated polymers (**M–R**), derived from di- and mono-substituted acetylene. These are based on the known conjugated polymer, poly[1-phenyl-2-(*p*-trimethylsilyl)phenylacetylene], which was previously demonstrated to be porous.[27]

After purification (see details in Supporting Information) followed by anti-solvent precipitation (by dissolving in dichloromethane (DCM) or in toluene and rapid precipitation into excess methanol), all polymers were isolated as powders that were found to be freely soluble in common organic solvents such as tetrahydrofuran (THF), DCM, chloroform, and toluene. All materials form polymer films after solvent evaporation. The materials were characterized by ^{1}H NMR, elemental microanalysis, and gel permeation chromatography (GPC). GPC demonstrated that these polymers have a range of average molar masses relative to polystyrene standards (Table 1). Absorption and emission spectra for linear polypyrenes, both in solution and cast as thin films, showed a blue-shift with respect to branched pyrene SCMPs (Figure S19, S20, Supporting Information),[13] and insoluble pyrene CMP networks,[28] as would be expected from the absence of macrocycles in the linear polymers.[15b]

The nitrogen adsorption isotherms were broadly similar for all polymers, each showing a type I or type II nitrogen isotherm (except **P** and **R**, see below) with a clear micropore step at low relative pressures. As an example, the highest and the lowest molecular weight samples of the linear 1,3-polypyrenes (**A** and **D**) are shown in **Figure 1** (see Figure S2, Supporting Information, for polymers **B** and **C**). The upturn in the nitrogen isotherm at higher relative pressures indicates meso/macroporosity, presumably from the nanoscopic particles and associated interparticle voids. The SA_{BET} of these polymers increases with the weight-averaged molecular weight from 400 to 728 m^2 g^{-1} with a pore size distribution in the micropore (<2 nm) range (Figure S3, Supporting Information). It is clear that the highest molecular weight polymer, **D**, has a significantly higher pore volume than the lower molecular weight analogues, **A–C** (Figure S4, Supporting Information).

Microporosity is also maintained when the backbones of the linear polymers are changed by inducing biphenyl groups or perylenediimidyl groups into the polymer chains (**E–L**, Figures S5–S7, Supporting Information), and the polymers with higher molecular weight have higher surface areas (Figure S8, Supporting Information). However, microporosity in the polyacetylenes, **M–R**, was found to depend more on the chemical structure of the monomers than on the molecular weight. Microporosity was only observed when trimethylsilyl (TMS) or *tert*-butyl side groups were present (Figure S9, Supporting Information), and polymers **P** and **R** were found to be non-porous to nitrogen at 77 K.

Polymer **A** was also analyzed for the adsorption of other gases, and was shown to adsorb hydrogen at 77 K (3.5 mmol g^{-1} at 1 bar), and CO_2 (1.2 mmol g^{-1} at 1 bar) at 273 K (Figures S10, S11, Supporting Information). This suggests the possibility of selectively porous coatings, if these materials can be cast as smooth films, as demonstrated previously for branched SCMPs.[13] To test film-forming, a smooth film of polymer **D** was prepared by evaporation from DCM. Anti-solvent precipitation of **D** gives both discrete and aggregated spheres of <100 nm in diameter (**Figure 2**). These nanoscopic particle dimensions

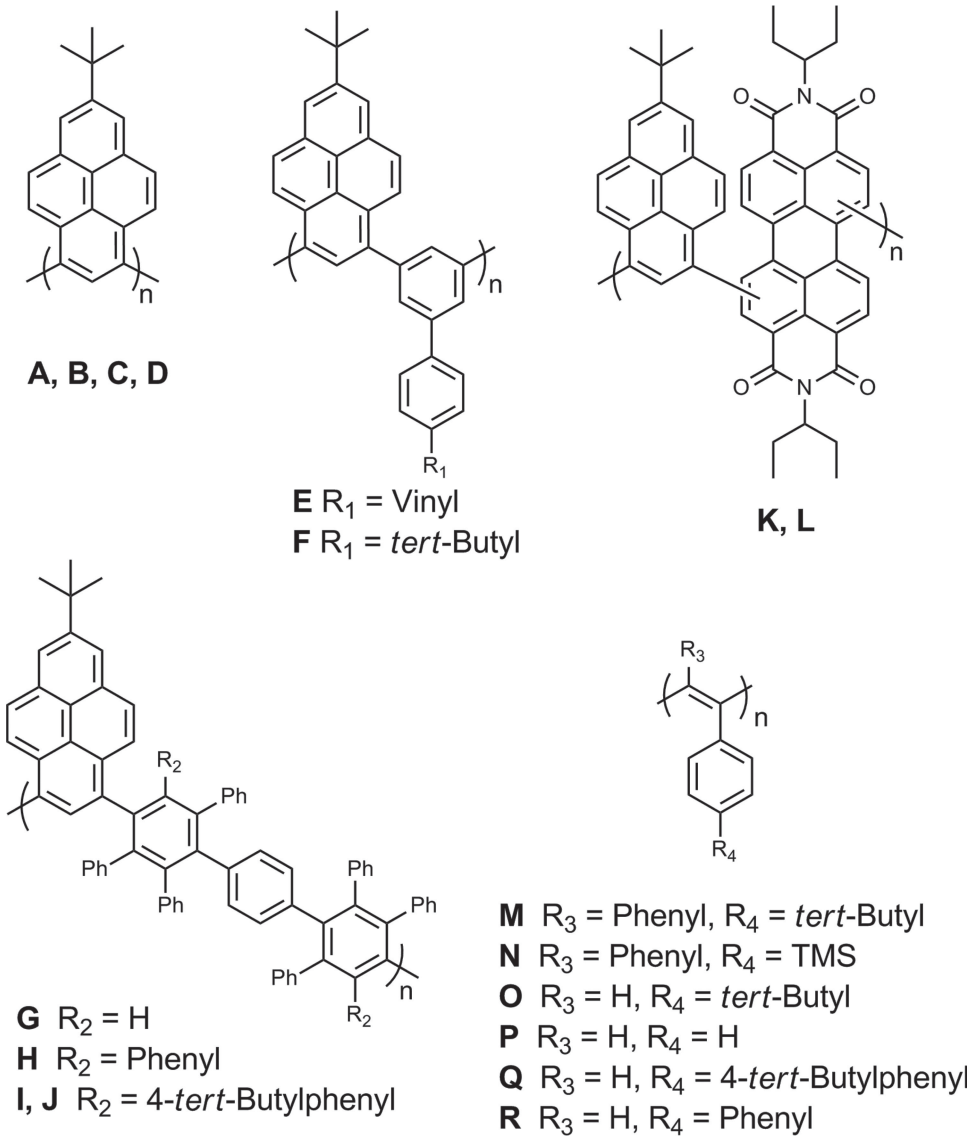

Scheme 1. Structures of the linear conjugated polymers of intrinsic microporosity prepared.

allow for rapid gas transport throughout the material, and account for the interparticulate macroporosity that is evidenced in sorption isotherms at high relative pressures (see above). The cast film of polymer **D**, however, was smooth and featureless (Figure 2, Figure S12, Supporting Information). Some of the films formed from branched pyrene SCMPs in our previous study[13] were found to be non-porous to nitrogen at 77 K. However, nitrogen porosity is maintained in the cast film of polymer **D**, although the nature of the isotherm was changed (**Figure 3**a). The total nitrogen uptake is similar to the precipitated material (cf., Figures 1, 3), but there is significantly more desorption hysteresis for the film, a slightly lower apparent SA_{BET} (686 vs. 728 $m^2 g^{-1}$), and a complete loss of the macroporous character that was exhibited by the precipitated, agglomerated powder sample of **D**. The slow gas adsorption kinetics in the film of polymer **D** made it necessary to increase the measurement equilibration time to 80 s, well above the 20 s that is

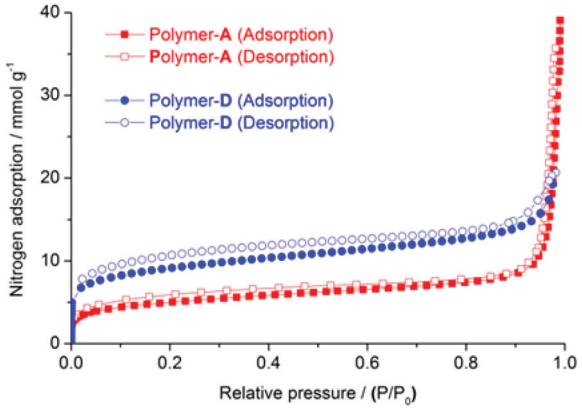

Figure 1. Nitrogen adsorption isotherms for polymer powders **A** (lowest M_w) and **D** (highest M_w), measured at 77 K up to 1 bar (desorption isotherms = open symbols).

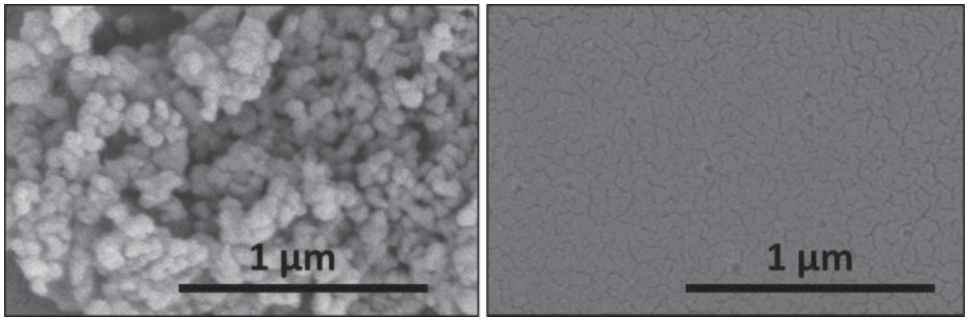

Figure 2. Scanning electron microscopy (SEM) images of precipitated (left) and cast films (right) of polymer **D** (M_w 8140 g mol^{-1}). Figure S12 (Supporting Information) shows a wider range of magnifications.

normally used. The apparent SA_{BET} recorded for these measurements was found to increase as a function of the equilibration time because faster measurements underestimate the gas uptake (Figure S13, Supporting Information). A higher value, closer to that of the precipitated particles of the same material, could potentially be achieved by increasing the equilibration times even further – as the results in Figure S13 do not reach a plateau. However, further increases in the equilibration time were avoided due to concerns over the stability/accuracy of these measurements over such long timescales. This behaviour indicates slow diffusion of nitrogen into/out of the polymer film of **D**, which lacks the macroporosity of the corresponding powder sample, at least at the measurement temperature of 77 K. Strong adsorption hysteresis is also common in isotherms recorded for cast films of non-conjugated PIMs.[29]

The hydrogen and nitrogen isotherms (at 77 K) for the cast film of polymer **D** are shown in Figure 3, along with CO_2 and N_2 isotherms at a higher temperature (273 K), where comparatively little hysteresis is observed. We also devised a strategy for crosslinking reactions based on polymer **E** by introducing pendant vinyl groups in the polymer chains. This allows the formation of crosslinked powder or crosslinked membranes that are stable to organic solvents. To create crosslinked powders, a homogeneous solution of polymer **E** in DCM was treated with Grubbs 2nd generation catalyst for 26 h at 55 °C under a nitrogen atmosphere. This produced an insoluble, crosslinked powder that maintained porosity to nitrogen (SA_{BET} = 607 m^2 g^{-1}; Figure S14, Supporting Information). To create crosslinked films, polymer **E** was first dissolved in DCM and then dip-coated as a uniform film on a glass slide, after which it was thermally crosslinked by heating at 250 °C for 4 h (the polymer itself is thermally stable up to ≈400 °C, Figure S15, Supporting Information). Before crosslinking, the polymer formed a uniform transparent and almost colorless film (**Figure 4**a, left). After thermal treatment, the crosslinked film remained uniform and transparent, but became insoluble and orange in color (Figure 4a, right, 4b). This crosslinked film lost porosity to nitrogen, while maintaining porosity to hydrogen and carbon dioxide (Figure S16, S17, Supporting Information), showing the potential to form selectively porous coatings. Indeed, with respect to the non-crosslinked film, thermal crosslinking increases the ideal CO_2/N_2 selectivity (at 1 bar, 100 000 Pa) from 5.8 (cast polymer **D**) to 9.4 (thermally crosslinked cast polymer **E**).

There is also the potential to tailor the porosity of the C-PIM films by directly modifying the structure of the monomers. For example, changing the structure between polymers **O** and **M** from a hydrogen to a phenyl group on the main-chain switches the respective films from non-porous to porous with respect to hydrogen (Figure S18, Supporting Information), most

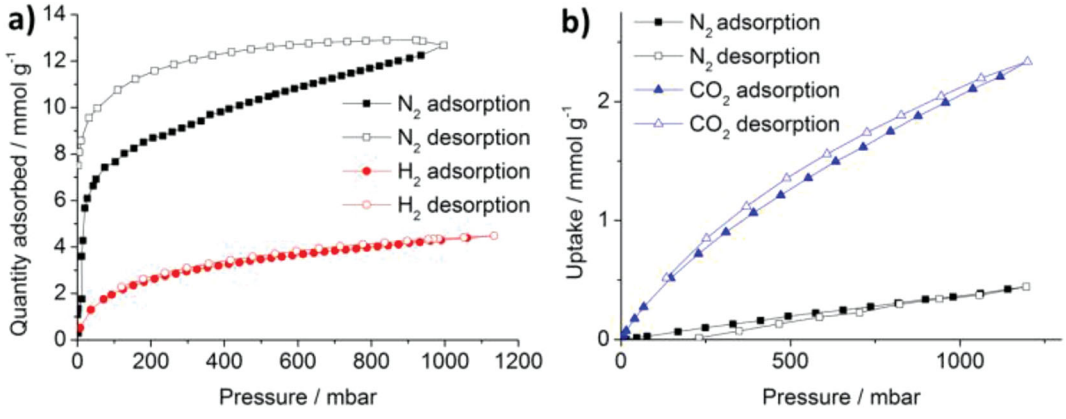

Figure 3. a) Nitrogen and hydrogen adsorption and desorption isotherms, at 77 K, of a cast film of polymer **D**. The nitrogen equilibration time was extended to 80 s. b) Carbon dioxide and nitrogen sorption isotherms for **D** at 273 K.

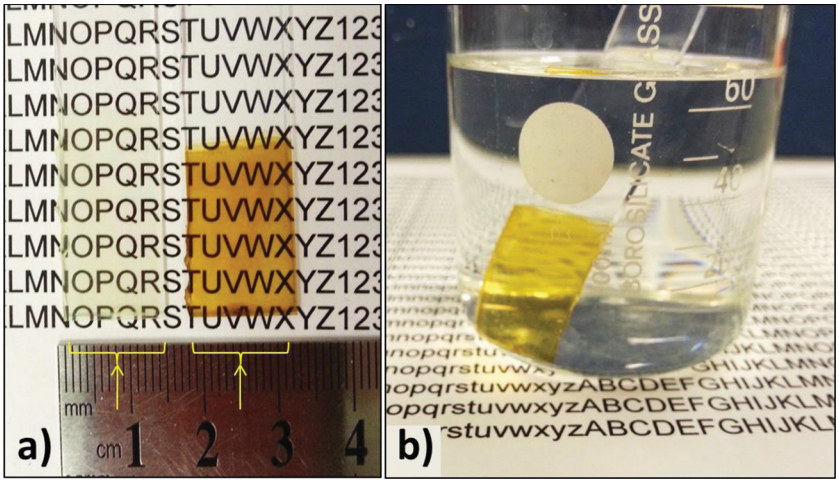

Figure 4. a) Dip-coated film of polymer **E** before (left) and after (right) thermal crosslinking. b) The crosslinked film is no longer soluble in dichloromethane.

likely because the additional steric bulk in the side chain of **M** increases the available free-volume in the film.

C-PIMs offer the possibility of introducing new physical properties that are not found in common membrane-forming polymers, nor in non-conjugated PIMs. For example, the difference in structure and conjugation for each of the polymers produces a range of different absorption/emission spectra for the materials. Solid state UV-visible and photoluminescence spectra for the full range of polymers, and representative photographs, are shown in Figures S19–S31, Supporting Information. Polymers **K** and **L**, in particular, have interesting photophysical properties, and polymer **L** has an optical band gap of 1.82 eV estimated from the absorption band edge (Figure S25, Supporting Information). Cyclic voltammetry for polymer **L** shows two quasi-reversible anodic peaks in the negative potential range, while no obvious redox peaks with positive potentials were detected (Figure S32, Supporting Information). This indicates that polymer **L** is a typical n-type material due to the strong electron withdrawing character of the perylenediimide moiety. In the negative potential, the $E_{1/2}$ are –0.96 and –0.26 V vs. $FeCp_2$. The LUMO energy level was estimated to be –6.05 eV[30] and, combined with the optical band gap, we estimate the HOMO energy level to be approximately –7.87 eV. We expect that the confluence of microporosity and electrochemical behavior in solution-processable conjugated polymers could allow the application of these new materials in organic electronic device fabrication.[31,32]

3. Conclusions

In summary, microporosity is attainable in a number of linear, soluble conjugated polymers, or C-PIMs, both using metal-mediated and metal-free synthesis routes. This is not limited to pyrene as a monomer, nor, importantly,[13] is hyperbranching a prerequisite for microporosity. Of the 18 structurally unique polymers presented in Table 1, 16 materials have substantial, permanent microporosity. We anticipate that a much larger number of additional C-PIMs remains to be discovered, and that this might encompass a broader range of functional monomers such as thiophenes, carbazoles, and the like. As in the case of non-conjugated PIMs, rigidity, contortion, and adequate molecular weight would seem to be the key design factors, although other effects are also important, such as the need for certain side groups to impart microporosity in the polyacetylenes, **M**–**R**. A number of challenges remain. For example, PIM-1, probably because of its spiroalkane linkages, maintains enough flexibility to combine permanent microporosity with reasonable mechanical properties. Hence, PIM-1 can form self-standing albeit somewhat brittle films, and this is not a feature that is trivial to combine with permanent microporosity. While we have not carried out detailed mechanical tests for polymers **A**–**R**, they form, in general, films with ductility that appears lower than for high-molecular weight PIM-1, although films of C-PIMs **A**–**R** are quite stable, in that they do not crack or peel off, when cast upon a suitable inflexible support. Mechanical strength may be important, for instance, in gas separations at higher pressures and flow rates, where membrane failure is a possible issue for more brittle materials. As such, the development of next-generation C-PIMs with better mechanical properties is a desirable research target. However, we also envisage different applications for C-PIMs that exploit the conjugated nature of the materials and associated photophysical or electrochemical properties. For example, solution-processable C-PIMs could conceivably be used as materials for electrochemical sensing, as printable organic supercapacitors,[8] or as high surface area components in devices for photochemical water splitting. In each case, the unique combination of permanent porosity, processability, and extended conjugation might offer new technologies, even in the absence of more robust mechanical properties.

4. Experimental Section

Typical synthesis method for linear 1,3-polypyrenes (e.g., **C**) via Suzuki coupling: To an oven-dried 50 mL flask equipped with a condenser and a magnetic stirring bar was charged the monomer 3-bromo-7-*tert*-butylpyrene-1-boronic acid pinacol ester (250 mg, 0.54 mmol), dioxane (12 mL), and toluene (4 mL), and a solution of K_3PO_4 (468 mg, 2.21 mmol) in H_2O (3 mL) was added. After degassing by freeze-pump-thaw cycles, $Pd(OAc)_2$ (4.4 mg, 0.02 mmol) and P(*o*-toyl)$_3$ (36.5 mg, 0.12 mmol) were added. The mixture was degassed again and stirred at 90 °C for 72 h. After cooling to room temperature, the mixture was diluted with dichloromethane, washed with 20% HCl solution, brine, and water, respectively, and dried over $MgSO_4$. The organic layer was filtered and evaporated to dryness. The crude product was purified with a short silica column (10 g), which was eluted with a gradient of dichloromethane/hexane (from 0 to 18%) until oligomers were removed, then changed to dichloromethane to elute the polymer. The solution was concentrated and filtered through a 0.2 μm syringe filter, followed by precipitation into methanol, and dried at 150 °C to give a yellow powder (62 mg) in 45% yield. GPC analysis: M_n = 3970 g mol^{-1}, M_w = 4910 g mol^{-1} and PDI = 1.24; ^{1}H NMR (400 MHz; $CDCl_3$; ppm) δ : 8.7–7.0 (brs, 7H),

1.57 (brs, 9H); Anal. Calc. for $(C_{20}H_{18})_n$: C, 92.98; H, 7.02. Found: C, 91.28; H 6.25.

Electron Microscopy: Samples were imaged using a Hitachi S-4800 cold field emission scanning electron microscope (FE-SEM) operating in scanning modes. Samples were prepared by depositing dry samples on 15 mm Hitachi M4 aluminum stubs using an adhesive high purity carbon tab before coating with a 2 nm layer of gold using an Emitech K550X automated sputter coater. Imaging was conducted at a working distance of 8 mm and a working voltage of 3 kV using a mix of upper and lower secondary electron detectors.

Gas Sorption Analysis: Surface areas were measured by nitrogen adsorption and desorption at 77.3 K. Powder samples were degassed offline at 110 °C for 15 h under dynamic vacuum (10^{-5} bar) before analysis. Isotherms were measured using a Micromeritics 2020, or 2420 volumetric adsorption analyzer. Surface areas were calculated in the relative pressure (P/P_0) range from 0.01 to 0.10 of the adsorption branch.

Supporting Information

Supporting Information is available from the Wiley Online Library or from the author.

Acknowledgements

The authors gratefully acknowledge EPSRC for funding (EP/H000925/1), and R. Clowes for assistance with sorption measurement. A.I.C. is a Royal Society Wolfson award holder.

Received: March 28, 2014
Published online: June 24, 2014

[1] J.-X. Jiang, F. Su, A. Trewin, C. D. Wood, N. L. Campbell, H. Niu, C. Dickinson, A. Y. Ganin, M. J. Rosseinsky, Y. Z. Khimyak, A. I. Cooper, *Angew. Chem. Int. Ed.* **2007**, *46*, 8574.
[2] L. Chen, Y. Yang, D. Jiang, *J. Am. Chem. Soc.* **2010**, *132*, 9138.
[3] L. Chen, Y. Honsho, S. Seki, D. Jiang, *J. Am. Chem. Soc.* **2010**, *132*, 6742.
[4] W. Lu, J. P. Sculley, D. Yuan, R. Krishna, Z. Wei, H.-C. Zhou, *Angew. Chem. Int. Ed.* **2012**, *51*, 7480.
[5] A. Li, H.-X. Sun, D.-Z. Tan, W.-J. Fan, S.-H. Wen, X.-J. Qing, G.-X. Li, S.-Y. Li, W.-Q. Deng, *Energy Environ. Sci.* **2011**, *4*, 2062.
[6] Y. Xu, L. Chen, Z. Guo, A. Nagai, D. Jiang, *J. Am. Chem. Soc.* **2011**, *133*, 17622.
[7] X. Liu, Y. Xu, D. Jiang, *J. Am. Chem. Soc.* **2012**, *134*, 8738.
[8] Y. Kou, Y. H. Xu, Z. Q. Guo, D. L. Jiang, *Angew. Chem. Int. Ed.* **2011**, *50*, 8753.
[9] a) T. Ben, H. Ren, S. Ma, D. Cao, J. Lan, X. Jing, W. Wang, J. Xu, F. Deng, J. M. Simmons, S. Qiu, G. Zhu, *Angew. Chem. Int. Ed.* **2009**, *48*, 9457; b) D. Yuan, D. Zhao, D. Sun, H.-C. Zhou, *Angew. Chem. Int. Ed.* **2010**, *49*, 5357.
[10] a) A. Patra, J.-M. Koenen, U. Scherf, *Chem. Commun.* **2011**, *47*, 9612; b) X. Wu, H. Li, Y. Xu, B. Xu, H. Tong, L. Wang, *Nanoscale* **2014**, *6*, 2375.
[11] X. Zhu, C. Tian, S. M. Mahurin, S.-H. Chai, C. Wang, S. Brown, G. M. Veith, H. Luo, H. Liu, S. Dai, *J. Am. Chem. Soc.* **2012**, *134*, 10478.
[12] P. M. Budd, B. S. Ghanem, S. Makhseed, N. B. McKeown, K. J. Msayib, C. E. Tattershall, *Chem. Commun.* **2004**, 230.
[13] G. Cheng, T. Hasell, A. Trewin, D. J. Adams, A. I. Cooper, *Angew. Chem. Int. Ed.* **2012**, *51*, 12727.
[14] T. M. Figueira-Duarte, S. C. Simon, M. Wagner, S. I. Drtezhinin, K. A. Zachariasse, K. Müllen, *Angew. Chem. Int. Ed.* **2008**, *47*, 10175.
[15] a) T. M. Figueira-Duarte, P. G. Del Rosso, R. Trattnig, S. Sax, E. J. W. List, K. Müllen, *Adv. Mater.* **2010**, *22*, 990; b) M. A. Zwijnenburg, G. Cheng, T. O. McDonald, K. E. Jelfs, J.-X. Jiang, S. Ren, T. Hasell, F. Blanc, A. I. Cooper, D. J. Adams, *Macromolecules* **2013**, *46*, 7696.
[16] N. B. McKeown, P. M. Budd, *Chem. Soc. Rev.* **2006**, *35*, 675.
[17] M. Carta, K. J. Msayib, P. M. Budd, N. B. McKeown, *Org. Lett.* **2008**, *10*, 2641.
[18] R. Short, M. Carta, C. G. Bezzu, D. Fritsch, B. M. Kariuki, N. B. McKeown, *Chem. Commun.* **2011**, *47*, 6822.
[19] B. S. Ghanem, M. Hashem, K. D. M. Harris, K. J. Msayib, M. Xu, P. M. Budd, N. Chaukura, D. Book, S. Tedds, A. Walton, N. B. McKeown, *Macromolecules* **2010**, *43*, 5287.
[20] N. B. McKeown, B. Gahnem, K. J. Msayib, P. M. Budd, C. E. Tattershall, K. Mahmood, S. Tan, D. Book, H. W. Langmi, A. Walton, *Angew. Chem. Int. Ed.* **2006**, *45*, 1804.
[21] G. Li, V. Shrotriya, J. S. Huang, Y. Yao, T. Moriarty, K. Emery, Y. Yang, *Nat. Mater.* **2005**, *4*, 864.
[22] a) R. H. Friend, R. W. Gymer, A. B. Holmes, J. H. Burroughes, R. N. Marks, C. Taliani, D. D. C. Bradley, D. A. Dos Santos, J. L. Brédas, M. Logdlund, W. R. Salaneck, *Nature* **1999**, *397*, 121; b) S. Guenes, H. Neugebauer, N. S. Sariciftci, *Chem. Rev.* **2007**, *107*, 1324; c) D. T. McQuade, A. E. Pullen, T. M. Swager, *Chem. Rev.* **2000**, *100*, 2537.
[23] M. Lv, S. Li, J. J. Jasieniak, J. Hou, J. Zhu, Z. A. Tan, S. E. Watkins, Y. Li, X. Chen, *Adv. Mater.* **2013**, *25*, 6889.
[24] J. Sakamoto, M. Rehahn, G. Wegner, A. D. Schlüter, *Macromol. Rapid Commun.* **2009**, *30*, 653.
[25] T. Yamamoto, S. Wakabayashi, K. Osakada, *J. Organomet. Chem.* **1992**, *428*, 223.
[26] a) O. Diels, K. Alder, *Liebigs Ann. Chem.* **1928**, *460*, 98; b) U. Kumar, T. X. Neenan, *Macromolecules* **1995**, *28*, 124; c) F. Morgenroth, E. Reuther, K. Müllen, *Angew. Chem. Int. Ed.* **1997**, *36*, 631.
[27] W.-E. Lee, D.-C. Han, D.-H. Han, H.-J. Choi, T. Sakaguchi, C.-L. Lee, G. Kwak, *Macromol. Rapid Commun.* **2011**, *32*, 1047.
[28] J. X. Jiang, A. Trewin, D. J. Adams, A. I. Cooper, *Chem. Sci.* **2011**, *2*, 1777.
[29] J. Jeromenok, J. Weber, *Langmuir* **2013**, *29*, 12982.
[30] C. M. Cardona, W. Li, A. E. Kaifer, D. Stockdale, G. C. Bazan, *Adv. Mater.* **2011**, *23*, 2367.
[31] C. Gu, Y. Chen, Z. Zhang, S. Xue, S. Sun, K. Zhang, C. Zhong, H. Zhang, Y. Pan, Y. Lv, Y. Yang, F. Li, S. Zhang, F. Huang, Y. Ma, *Adv. Mater.* **2013**, *25*, 3443.
[32] F. Vilela, K. Zhang, M. Antonietti, *Energy Environ. Sci.* **2012**, *5*, 7819.